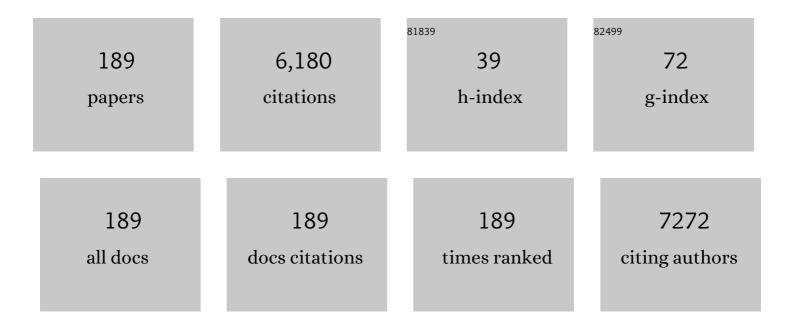
List of Publications by Year in descending order

Source: https://exaly.com/author-pdf/9151426/publications.pdf Version: 2024-02-01



#	Article	IF	CITATIONS
1	Plasma-enhanced atomic layer deposition of nickel and cobalt phosphate for lithium ion batteries. Dalton Transactions, 2022, 51, 2059-2067.	1.6	3
2	Spectroscopic Ellipsometry for Operando Monitoring of (De)Lithiation-Induced Phenomena on LiMn <sub>2</sub> O <sub>4</sub> and LiNi <sub>0.5</sub> Mn <sub>1.5</sub> O <sub>4</sub> Electrodes. Journal of the Electrochemical Society, 2022, 169, 040501.	1.3	3
3	Titanium Carboxylate Molecular Layer Deposited Hybrid Films as Protective Coatings for Lithium-Ion Batteries. ACS Applied Materials & Interfaces, 2022, 14, 24908-24918.	4.0	4
4	(Invited) Electrochemically Induced Deposition of Thin-Film Oxides and Electronic Insulators. ECS Meeting Abstracts, 2022, MA2022-01, 1129-1129.	0.0	0
5	In-depth study of structural, morphological and electronic changes during conversion and alloying of ITO. Journal of Materials Chemistry A, 2021, 9, 10447-10457. Surpassing the Tu/Tr capacity limit in chlorine modified TIO (mml:math	5.2	3
6	xmlns:mml="http://www.w3.org/1998/Math/MathML" altimg="si10.svg"> <mml:msub><mml:mrow /&gt;<mml:mrow><mml:mn>2</mml:mn><mml:mo>â^'</mml:mo><mml:mi mathvariant="normal"&gt;y</mml:mi </mml:mrow></mml:mrow </mml:msub> Cl <mml:math xmlns:mml="http://www.w3.org/1998/Math/MathML" altimg="si11.svg"&gt;<mml:msub><mml:mrow /&gt;<mml:mrow><mml:mn>2<td>9.5</td><td>4</td></mml:mn></mml:mrow></mml:mrow </mml:msub></mml:math 	9.5	4
7	mathyainat="mormal">>>>> Plasma enhanced atomic layer deposition of a (nitrogen doped) Ti phosphate coating for improved energy storage in Li-ion batteries. Journal of Power Sources, 2021, 497, 229866.	4.0	8
8	Interfacial Conductivity Enhancement and Pore Confinement Conductivity-Lowering Behavior inside the Nanopores of Solid Silica-gel Nanocomposite Electrolytes. ACS Applied Materials & Interfaces, 2021, 13, 40543-40551.	4.0	9
9	Aggregate-Free Micrometer-Thick Mesoporous Silica Thin Films on Planar and Three-Dimensional Structured Electrodes by Hydrodynamic Diffusion Layer Control during Electrochemically Assisted Self-Assembly. Chemistry of Materials, 2021, 33, 7075-7088.	3.2	7
10	The Role of Electronic Junctions in Artificial Interface Engineering: The Case for Indium Tin Oxide on LiMn <sub>2</sub> O <sub>4</sub> Electrodes. Advanced Functional Materials, 2021, 31, 2105180.	7.8	3
11	Effect of different oxide and hybrid precursors on MOF-CVD of ZIF-8 films. Dalton Transactions, 2021, 50, 6784-6788.	1.6	13
12	Detrimental MnPO <sub>4</sub> F and MnF <sub>2</sub> formation on LiMn <sub>2</sub> O <sub>4</sub> in the 3 V region. Journal of Materials Chemistry A, 2021, 9, 23256-23268.	5.2	7
13	An IR Spectroscopy Study of the Degradation of Surface Bound Azido-Groups in High Vacuum. Langmuir, 2021, 37, 12608-12615.	1.6	2
14	Implementation of Dual Number Automatic Differentiation with John Newman's BAND Algorithm. Journal of the Electrochemical Society, 2021, 168, 113501.	1.3	0
15	Interphase Control for Electrodeposition of Thin Lithium Films for Lithium Metal Batteries. ECS Meeting Abstracts, 2021, MA2021-02, 734-734.	0.0	0
16	(Invited) The Role of Surface Inhibition in Deterministic Controlled Electrodeposition. ECS Meeting Abstracts, 2021, MA2021-02, 695-695.	0.0	0
17	Asymmetric Li-Ion Diffusion Profiles during Lithium Plating and Stripping in Ionic Liquid Electrolytes. ECS Meeting Abstracts, 2021, MA2021-02, 719-719.	0.0	0
18	Asymmetric Impact of External Pressure on Li/Solid-Electrolyte Interfacial Stability. ECS Meeting Abstracts. 2021. MA2021-02. 731-731.	0.0	0

#	Article	IF	CITATIONS
19	Silica gel solid nanocomposite electrolytes with interfacial conductivity promotion exceeding the bulk Li-ion conductivity of the ionic liquid electrolyte filler. Science Advances, 2020, 6, eaav3400.	4.7	51
20	Pore structure analysis of ionic liquid-templated porous silica using positron annihilation lifetime spectroscopy. Microporous and Mesoporous Materials, 2020, 295, 109964.	2.2	4
21	Molecular Layer Deposition of "Magnesiconeâ€; a Magnesium-based Hybrid Material. Chemistry of Materials, 2020, 32, 4451-4466.	3.2	17
22	Atomic Layer Deposition of Nitrogen-Doped Al Phosphate Coatings for Li-Ion Battery Applications. ACS Applied Materials & Interfaces, 2020, 12, 25949-25960.	4.0	14
23	High-Rate Performance Solid-State Lithium Batteries with Silica-Gel Solid Nanocomposite Electrolytes using Bis(fluorosulfonyl)imide-Based Ionic Liquid. Journal of the Electrochemical Society, 2020, 167, 070549.	1.3	7
24	Amorphous MnO <sub>2</sub> Coated 3D Ni Nanomesh as a Thin-film Hybrid Cathode Material under O <sub>2</sub> Atmosphere. Journal of the Electrochemical Society, 2020, 167, 020507.	1.3	3
25	Interconnected Ni nanowires integrated with Li <sub>x</sub> MnO <sub>2</sub> as fast charging and high volumetric capacity cathodes for Li-ion batteries. Journal of Materials Chemistry A, 2020, 8, 14178-14189.	5.2	5
26	Advances in 3D Thinâ€Film Liâ€Ion Batteries. Advanced Materials Interfaces, 2019, 6, 1900805.	1.9	88
27	3D LiMn <sub>2</sub> O <sub>4</sub> thin-film electrodes for high rate all solid-state lithium and Li-ion microbatteries. Journal of Materials Chemistry A, 2019, 7, 18996-19007.	5.2	25
28	A Highâ€Surfaceâ€Area Carbon oated 3D Nickel Nanomesh for Li–O 2 Batteries. ChemSusChem, 2019, 12, 3967-3970.	3.6	5
29	Integrated Cleanroom Process for the Vapor-Phase Deposition of Large-Area Zeolitic Imidazolate Framework Thin Films. Chemistry of Materials, 2019, 31, 9462-9471.	3.2	52
30	Copper Rich Cu <sub>1-x</sub> Ni <sub>x</sub> Alloys (0.05 < x < 0.15) Electrodeposited from Acid Sulfate-Based Electrolyte with Benzotriazole Additive for Microbump Metallization for 3D Stacked Integrated Circuits. Journal of the Electrochemical Society, 2019, 166, D315-D322.	1.3	1
31	Redox Layer Deposition of Thin Films of MnO <sub>2</sub> on Nanostructured Substrates from Aqueous Solutions. Chemistry of Materials, 2019, 31, 4805-4816.	3.2	18
32	Electrochemical Determination of Porosity and Surface Area of Thin Films of Interconnected Nickel Nanowires. Journal of the Electrochemical Society, 2019, 166, D227-D235.	1.3	28
33	Plasma-Assisted ALD of LiPO(N) for Solid State Batteries. Journal of the Electrochemical Society, 2019, 166, A1239-A1242.	1.3	26
34	Effect of high temperature LiPON electrolyte in all solid state batteries. Solid State Ionics, 2019, 337, 24-32.	1.3	32
35	Toward 3D Thin-Film Batteries: Optimal Current-Collector Design and Scalable Fabrication of TiO <sub>2</sub> Thin-Film Electrodes. ACS Applied Energy Materials, 2019, 2, 1774-1783.	2.5	23
36	Novel Thinâ€Film Solid Nanocomposite Electrolyte for Lithiumâ€Ion Batteries by Combined MLD and ALD. Advanced Materials Interfaces, 2019, 6, 1901407.	1.9	5

#	Article	IF	CITATIONS
37	Investigation of the Li-Ion Insertion Mechanism for Amorphous and Anatase TiO <sub>2</sub> Thin-Films. Journal of the Electrochemical Society, 2019, 166, A1-A9.	1.3	44
38	Differential Inhibition during Cu Electrodeposition on Ru: Combined Electrochemical and Real-Time TEM Studies. Journal of the Electrochemical Society, 2019, 166, D3129-D3135.	1.3	9
39	Solid and Solidâ€Like Composite Electrolyte for Lithium Ion Batteries: Engineering the Ion Conductivity at Interfaces. Advanced Materials Interfaces, 2019, 6, 1800899.	1.9	72
40	On the chemistry and electrochemistry of LiPON breakdown. Journal of Materials Chemistry A, 2018, 6, 4848-4859.	5.2	44
41	The transformation behaviour of "aluconesâ€ <del>,</del> deposited by molecular layer deposition, in nanoporous Al <sub>2</sub> O <sub>3</sub> layers. Dalton Transactions, 2018, 47, 5860-5870.	1.6	40
42	Combining High Porosity with High Surface Area in Flexible Interconnected Nanowire Meshes for Hydrogen Generation and Beyond. ACS Applied Materials & Interfaces, 2018, 10, 44634-44644.	4.0	20
43	Bending impact on the performance of a flexible Li <sub>4</sub> Ti <sub>5</sub> O <sub>12</sub> -based all-solid-state thin-film battery. Science and Technology of Advanced Materials, 2018, 19, 454-464.	2.8	44
44	Continuous and Conformal Lithium Titanate Spinel Thin Films by Solid State Reaction. Journal of the Electrochemical Society, 2018, 165, B3184-B3193.	1.3	8
45	Direct imaging and manipulation of ionic diffusion in mixed electronic–ionic conductors. Nanoscale, 2018, 10, 12564-12572.	2.8	5
46	Nanoscale electrochemical response of lithium-ion cathodes: a combined study using C-AFM and SIMS. Beilstein Journal of Nanotechnology, 2018, 9, 1623-1628.	1.5	10
47	Heterogeneous TiO <sub>2</sub> /V <sub>2</sub> O <sub>5</sub> /Carbon Nanotube Electrodes for Lithium-Ion Batteries. ACS Applied Materials & Interfaces, 2017, 9, 8055-8064.	4.0	32
48	Nanometer-Thin Graphitic Carbon Buffer Layers for Electrolytic MnO <sub>2</sub> for Thin-Film Energy Storage Devices. Journal of the Electrochemical Society, 2017, 164, A538-A544.	1.3	5
49	Analysis of Fully On-Chip Microfluidic Electrochemical Systems under Laminar Flow. Electrochimica Acta, 2017, 231, 200-208.	2.6	9
50	Plasma - Assisted ALD of Lipo(N) for Solid State Batteries. ECS Transactions, 2017, 75, 61-69.	0.3	15
51	The Influence of Ultrathin Amorphous ALD Alumina and Titania on the Rate Capability of Anatase TiO <sub>2</sub> and LiMn <sub>2</sub> O <sub>4</sub> Lithium Ion Battery Electrodes. Advanced Materials Interfaces, 2017, 4, 1601237.	1.9	50
52	100 nm Thinâ€Film Solidâ€Composite Electrolyte for Lithiumâ€Ion Batteries. Advanced Materials Interfaces, 2017, 4, 1600877.	1.9	6
53	Plasma-assisted and thermal atomic layer deposition of electrochemically active Li <sub>2</sub> CO <sub>3</sub> . RSC Advances, 2017, 7, 41359-41368.	1.7	38
54	Plasma-enhanced atomic layer deposition of vanadium phosphate as a lithium-ion battery electrode material. Journal of Vacuum Science and Technology A: Vacuum, Surfaces and Films, 2017, 35, .	0.9	12

#	Article	IF	CITATIONS
55	A USB-controlled potentiostat/galvanostat for thin-film battery characterization. HardwareX, 2017, 2, 34-49.	1.1	76
56	Effects of laminar flow within a versatile microfluidic chip for in-situ electrode characterization and fuel cells. Microelectronic Engineering, 2017, 181, 47-54.	1.1	8
57	Electrodeposition of Adherent Submicron to Micron Thick Manganese Dioxide Films with Optimized Current Collector Interface for 3D Li-Ion Electrodes. Journal of the Electrochemical Society, 2017, 164, D954-D963.	1.3	14
58	Chlorine Doping of Amorphous TiO <sub>2</sub> for Increased Capacity and Faster Li <sup>+</sup> -lon Storage. Chemistry of Materials, 2017, 29, 10007-10018.	3.2	46
59	Electrodeposition of insulating poly(phenylene oxide) films with variable thickness. Journal of Applied Polymer Science, 2017, 134, .	1.3	3
60	Plasma-enhanced atomic layer deposition of titanium phosphate as an electrode for lithium-ion batteries. Journal of Materials Chemistry A, 2017, 5, 330-338.	5.2	31
61	Electrolytic Manganese Dioxide Coatings on High Aspect Ratio Micro-Pillar Arrays for 3D Thin Film Lithium Ion Batteries. Nanomaterials, 2017, 7, 126.	1.9	9
62	Height Uniformity of Micro-Bumps Electroplated on Thin Cu Seed Layers. ECS Transactions, 2016, 72, 145-152.	0.3	2
63	Towards metal–organic framework based field effect chemical sensors: UiO-66-NH <sub>2</sub> for nerve agent detection. Chemical Science, 2016, 7, 5827-5832.	3.7	108
64	Plasma-enhanced atomic layer deposition of zinc phosphate. Journal of Non-Crystalline Solids, 2016, 444, 43-48.	1.5	17
65	Plasma-Enhanced Atomic Layer Deposition of Iron Phosphate as a Positive Electrode for 3D Lithium-Ion Microbatteries. Chemistry of Materials, 2016, 28, 3435-3445.	3.2	44
66	Electro-precipitation via oxygen reduction: a new technique for thin film manganese oxide deposition. Journal of Materials Chemistry A, 2016, 4, 13555-13562.	5.2	2
67	The Effect of the Substrate Characteristics on the Electrochemical Nucleation and Growth of Copper. Journal of the Electrochemical Society, 2016, 163, D3053-D3061.	1.3	8
68	Chemical vapour deposition of zeolitic imidazolate framework thinÂfilms. Nature Materials, 2016, 15, 304-310.	13.3	528
69	Electrical Characterization of Ultrathin RF-Sputtered LiPON Layers for Nanoscale Batteries. ACS Applied Materials & Interfaces, 2016, 8, 7060-7069.	4.0	63
70	Molecular layer deposition of "titaniconeâ€; a titanium-based hybrid material, as an electrode for lithium-ion batteries. Dalton Transactions, 2016, 45, 1176-1184.	1.6	45
71	The Formation Mechanism of 3D Porous Anodized Aluminum Oxide Templates from an Aluminum Film with Copper Impurities. Journal of Physical Chemistry C, 2015, 119, 2105-2112.	1.5	30
72	Self-limiting electropolymerization of ultrathin, pinhole-free poly(phenylene oxide) films on carbon nanosheets. Carbon, 2015, 88, 42-50.	5.4	21

#	Article	IF	CITATIONS
73	Deposition of MnO Anode and MnO <sub>2</sub> Cathode Thin Films by Plasma Enhanced Atomic Layer Deposition Using the Mn(thd) <sub>3</sub> Precursor. Chemistry of Materials, 2015, 27, 3628-3635.	3.2	40
74	High Cycling Stability and Extreme Rate Performance in Nanoscaled LiMn <sub>2</sub> O <sub>4</sub> Thin Films. ACS Applied Materials & Interfaces, 2015, 7, 22413-22420.	4.0	59
75	The Limitation and Optimization of Bottom-Up Growth Mode in Through Silicon Via Electroplating. Journal of the Electrochemical Society, 2015, 162, D599-D604.	1.3	15
76	An ELISA-based amperometric biosensor within a photo-patternable adhesive microfluidic channel. , 2015, , .		1
77	Characterization of thin films of the solid electrolyte Li <sub>x</sub> Mg <sub>1â^2x</sub> Al <sub>2+x</sub> O <sub>4</sub> (x = 0, 0.05, 0.15, 0.25). Physical Chemistry Chemical Physics, 2015, 17, 29045-29056.	1.3	8
78	Dual Role of Hydrogen in Low Temperature Plasma Enhanced Carbon Nanotube Growth. Journal of Physical Chemistry C, 2015, 119, 18293-18302.	1.5	8
79	Quantifying the Aggregation Factor in Carbon Nanotube Dispersions by Absorption Spectroscopy. Journal of Nanoscience, 2014, 2014, 1-13.	2.6	6
80	Electrodeposition and Characterization of Manganese Dioxide Thin Films on Silicon Pillar Arrays for 3D Thin-Film Lithium-Ion Batteries. ECS Transactions, 2014, 61, 29-41.	0.3	6
81	Stochastic Modeling of Polyethylene Glycol as a Suppressor in Copper Electroplating. Journal of the Electrochemical Society, 2014, 161, D269-D276.	1.3	30
82	Determination of elastic properties of a MnO2 coating by surface acoustic wave velocity dispersion analysis. Journal of Applied Physics, 2014, 116, .	1.1	28
83	Anodic Etching of n-GaN Epilayer into Porous GaN and Its Photoelectrochemical Properties. Journal of Physical Chemistry C, 2014, 118, 29492-29498.	1.5	72
84	Atomic Layer Deposition of Aluminum Phosphate Based on the Plasma Polymerization of Trimethyl Phosphate. Chemistry of Materials, 2014, 26, 6863-6871.	3.2	37
85	Nanostructured TiO <sub>2</sub> /carbon nanosheet hybrid electrode for high-rate thin-film lithium-ion batteries. Nanotechnology, 2014, 25, 504008.	1.3	39
86	(Invited) Wafer Scale Copper Direct Plating on Thin PVD RuTa Layers: A Route to Enable Filling 30 nm Features and Below. ECS Transactions, 2014, 58, 3-15.	0.3	1
87	Electrochemical Deposition of Manganese Oxides on Carbon Nanosheets. ECS Transactions, 2014, 61, 1-7.	0.3	1
88	The Effect of Polyether Suppressors on the Nucleation and Growth of Copper on RuTa Seeded Substrate for Direct Copper Plating. Electrochimica Acta, 2014, 127, 315-326.	2.6	10
89	Growth and integration challenges for carbon nanotube interconnects. Microelectronic Engineering, 2014, 120, 188-193.	1.1	20
90	Effect of Film Morphology on the Li Ion Intercalation Kinetics in Anodic Porous Manganese Dioxide Thin Films. Journal of Physical Chemistry C, 2014, 118, 9889-9898.	1.5	17

#	Article	IF	CITATIONS
91	Large Area Carbon Nanosheet Capacitors. ECS Solid State Letters, 2014, 3, N8-N10.	1.4	5
92	Synthesis of a 3D network of Pt nanowires by atomic layer deposition on a carbonaceous template. Nanoscale, 2014, 6, 6939.	2.8	14
93	Electrodeposition of Lithium from Lithium-Containing Solvate Ionic Liquids. Journal of Physical Chemistry C, 2014, 118, 20152-20162.	1.5	29
94	First-principles material modeling of solid-state electrolytes with the spinel structure. Physical Chemistry Chemical Physics, 2014, 16, 5399.	1.3	14
95	Atomic layer deposition-based synthesis of photoactive TiO2 nanoparticle chains by using carbon nanotubes as sacrificial templates. RSC Advances, 2014, 4, 11648.	1.7	48
96	Impact of Plasma-Induced Surface Damage on the Photoelectrochemical Properties of GaN Pillars Fabricated by Dry Etching. Journal of Physical Chemistry C, 2014, 118, 11261-11266.	1.5	12
97	Wafer Scale Copper Direct Plating on Thin PVD RuTa Layers: A Route to Enable Filling 30 nm Features and Below?. Journal of the Electrochemical Society, 2014, 161, D564-D570.	1.3	4
98	Electrochemical Deposition of Subnanometer Ni Films on TiN. Langmuir, 2014, 30, 2047-2053.	1.6	19
99	Effects of Counter Electrode Induced Redox Cycling on Fe(III) Reduction within Microfluidic Electrochemical Cells. Journal of the Electrochemical Society, 2014, 161, E128-E134.	1.3	9
100	Direct correlation between the measured electrochemical capacitance, wettability and surface functional groups of CarbonNanosheets. Electrochimica Acta, 2014, 132, 574-582.	2.6	36
101	Photocatalytic acetaldehyde oxidation in air using spacious TiO2 films prepared by atomic layer deposition on supported carbonaceous sacrificial templates. Applied Catalysis B: Environmental, 2014, 160-161, 204-210.	10.8	37
102	Direct Copper Plating. Nanostructure Science and Technology, 2014, , 131-173.	0.1	3
103	The Kinetics of Nanometer Sized TiO <sub>2</sub> Films as a Lithium-Ion Insertion Electrode. ECS Meeting Abstracts, 2014, MA2014-02, 478-478.	0.0	1
104	Solvent-free synthesis of supported ZIF-8 films and patterns through transformation of deposited zinc oxide precursors. CrystEngComm, 2013, 15, 9308.	1.3	124
105	Electrodeposition of Bismuth Telluride Thermoelectric Films from Chloride-Free Ethylene Glycol Solutions. Journal of the Electrochemical Society, 2013, 160, D196-D201.	1.3	19
106	Enhanced nucleation of Ni nanoparticles on TiN through H3BO3-mediated growth inhibition. Electrochimica Acta, 2013, 109, 411-418.	2.6	18
107	Wafer-scale Cu plating uniformity on thin Cu seed layers. Electrochimica Acta, 2013, 104, 242-248.	2.6	23
108	The effect of cupric ion concentration on the nucleation and growth of copper on RuTa seeded substrates. Electrochimica Acta, 2013, 92, 474-483.	2.6	22

#	Article	IF	CITATIONS
109	Synthesis of large area carbon nanosheets for energy storage applications. Carbon, 2013, 58, 59-65.	5.4	48
110	Electrical characterization of CNT contacts with Cu Damascene top contact. Microelectronic Engineering, 2013, 106, 106-111.	1.1	26
111	Selective Actuation of Arrays of Carbon Nanotubes Using Magnetic Resonance. ACS Nano, 2013, 7, 5777-5783.	7.3	4
112	Electrodeposition of Antimony, Tellurium and Their Alloys from Molten Acetamide Mixtures. Journal of the Electrochemical Society, 2013, 160, D75-D79.	1.3	15
113	(Invited) Conformal Deposition for 3D Thin-Film Batteries. ECS Transactions, 2013, 58, 111-118.	0.3	22
114	Enhanced Photocatalytic Activity of Nanoroughened GaN by Dry Etching. ECS Electrochemistry Letters, 2013, 2, H51-H53.	1.9	6
115	Ultra-Low Copper Baths for Sub-35 nm Copper Interconnects. Journal of the Electrochemical Society, 2013, 160, D3255-D3259.	1.3	5
116	Modeling the Bottom-Up Filling of Through-Silicon vias Through Suppressor Adsorption/Desorption Mechanism. Journal of the Electrochemical Society, 2013, 160, D3051-D3056.	1.3	76
117	Electrochemical Determination of the Cupric Ion Activity in Aqueous Acidic Cupric Sulfate Electrolytes. Journal of the Electrochemical Society, 2013, 160, D60-D65.	1.3	4
118	Enhanced Photoelectrochemical Activity of GaN by Dry Etching into Nanopillar Array. ECS Transactions, 2013, 53, 29-35.	0.3	2
119	Growth Mechanism of a Hybrid Structure Consisting of a Graphite Layer on Top of Vertical Carbon Nanotubes. Journal of Nanomaterials, 2012, 2012, 1-10.	1.5	7
120	Nucleation and Growth of Copper on Ru-Based Substrates: II. The Effect of the Suppressor Additive. ECS Transactions, 2012, 41, 99-110.	0.3	9
121	Nucleation and Growth of Copper on Ru-Based Substrates: I. The Effect of the Inorganic Components. ECS Transactions, 2012, 41, 75-82.	0.3	6
122	Ultra-Low Copper Baths for Sub-35nm Copper Interconnects. ECS Transactions, 2012, 41, 83-97.	0.3	5
123	Strain relaxation in GaN nanopillars. Applied Physics Letters, 2012, 101, .	1.5	19
124	Growth of carbon nanotube branches by electrochemical decoration of carbon nanotubes. Materials Letters, 2012, 88, 33-35.	1.3	6
125	Multi-scale modeling of direct copper plating on resistive non-copper substrates. Electrochimica Acta, 2012, 78, 524-531.	2.6	18
126	Electrical and structural characterization of 150 nm CNT contacts with Cu damascene top metallization. , 2012, , .		2

#	Article	IF	CITATIONS
127	Carbon nanotube growth from Langmuir–Blodgett deposited Fe3O4nanocrystals. Nanotechnology, 2012, 23, 405604.	1.3	6
128	Correlation between number of walls and diameter in multiwall carbon nanotubes grown by chemical vapor deposition. Carbon, 2012, 50, 1748-1752.	5.4	60
129	Electrodeposition of bismuth telluride thermoelectric films from a nonaqueous electrolyte using ethylene glycol. Electrochimica Acta, 2012, 68, 9-17.	2.6	33
130	Adsorption/Desorption of Suppressor Complex on Copper: Description of the Critical Potential. ECS Transactions, 2011, 33, 13-26.	0.3	9
131	Measuring the electrical resistivity and contact resistance of vertical carbon nanotube bundles for application as interconnects. Nanotechnology, 2011, 22, 085302.	1.3	101
132	A study of Joule heating-induced breakdown of carbon nanotube interconnects. Nanotechnology, 2011, 22, 395202.	1.3	39
133	Carbon nanotube–carbon nanotube contacts as an alternative towards low resistance horizontal interconnects. Carbon, 2011, 49, 4004-4012.	5.4	30
134	Integration and electrical characterization of carbon nanotube via interconnects. Microelectronic Engineering, 2011, 88, 837-843.	1.1	58
135	Impact of "terminal effect―on Cu electrochemical deposition: Filling capability for different metallization options. Microelectronic Engineering, 2011, 88, 754-759.	1.1	22
136	Carbon nanotube interconnects: Electrical characterization of 150 nm CNT contacts with Cu damascene top contact. , 2011, , .		5
137	Measurement of Seebeck coefficient of electroplated thermoelectric films in presence of a seed layer. Journal of Materials Research, 2011, 26, 1953-1957.	1.2	10
138	ALD of Al2O3 for Carbon Nanotube vertical interconnect and its impact on the electrical properties. Materials Research Society Symposia Proceedings, 2011, 1283, 1.	0.1	8
139	Direct Copper Electrochemical Deposition on Ru-Based Substrates for Advanced Interconnects Target 30 nm and 1/2 Pitch Lines: From Coupon to Full-Wafer Experiments. ECS Transactions, 2011, 35, 117-123.	0.3	7
140	Copper Plating on Resistive Substrates, Diffusion Barrier and Alternative Seed Layers. ECS Transactions, 2010, 25, 175-184.	0.3	10
141	Impact of "Terminal Effect" on Cu Plating: Theory and Experimental Evidence. ECS Transactions, 2010, 25, 185-194.	0.3	15
142	Effect of the Ionic Strength and the Electrolyte Composition on the Suppression of Copper Deposition by PEG. ECS Transactions, 2010, 25, 67-78.	0.3	5
143	Investigation of Dimethyl Sulfoxide Electrolytes for Electrodepositing Thermoelectric Bismuth Telluride Films. ECS Transactions, 2010, 33, 75-80.	0.3	4
144	Integration of Vertical Carbon Nanotube Bundles for Interconnects. Journal of the Electrochemical Society, 2010, 157, K211.	1.3	26

#	Article	IF	CITATIONS
145	Tailoring Copper Island Density for Copper Plating on a RuTa Substrate. ECS Transactions, 2010, 28, 9-16.	0.3	3
146	Silver-Assisted Etching of Silicon Nanowires. ECS Transactions, 2010, 33, 49-58.	0.3	5
147	Growth and characterization of horizontally suspended CNTs across TiN electrode gaps. Nanotechnology, 2010, 21, 245604.	1.3	12
148	Electrochemical Tailoring of Catalyst Nanoparticles for CNT Spatial-Dimension Control. Journal of the Electrochemical Society, 2010, 157, K47.	1.3	9
149	Integration of Vertical Carbon Nanotube Bundles for Interconnects. ECS Transactions, 2009, 19, 11-24.	0.3	4
150	Growth and Electrical Characterization of Horizontally Aligned CNTs. ECS Transactions, 2009, 18, 845-850.	0.3	7
151	Stress in Electrodeposited High Moment CoFe Films. ECS Transactions, 2009, 25, 35-43.	0.3	0
152	Changing Superfilling Mode for Copper Electrodeposition in Blind Holes from Differential Inhibition to Differential Acceleration. Electrochemical and Solid-State Letters, 2009, 12, D39.	2.2	47
153	Copper Plating for 3D Interconnects. ECS Transactions, 2009, 25, 119-125.	0.3	4
154	Selective Growth of Carbon Nanotubes on Silicon from Electrodeposited Nickel Catalyst. Science of Advanced Materials, 2009, 1, 86-92.	0.1	8
155	Electrochemical Nucleation and Growth of Copper on Resistive Substrates. ECS Transactions, 2008, 11, 25-33.	0.3	4
156	Growth of carbon nanotubes as horizontal interconnects. Physica Status Solidi (B): Basic Research, 2008, 245, 2308-2310.	0.7	14
157	Reducing the electrodeposition time for filling microvias with copper for 3D technology. , 2008, , .		0
158	Electrodeposited Free-Standing Single-Crystal Indium Nanowires. Electrochemical and Solid-State Letters, 2008, 11, K47.	2.2	8
159	Effect of Additives on Shape Evolution during Electrodeposition. Journal of the Electrochemical Society, 2008, 155, D223.	1.3	22
160	Growth and Integration of High-Density CNT for BEOL Interconnects. Materials Research Society Symposia Proceedings, 2008, 1079, 1.	0.1	2
161	Etching of copper in deionized water rinse. , 2008, , .		4
162	Cu Plating of Through-Si Vias for 3D-Stacked Integrated Circuits. Materials Research Society Symposia Proceedings, 2008, 1112, 1.	0.1	1

#	Article	IF	CITATIONS
163	Size-Dependent Characteristics of Indium-Seeded Si Nanowire Growth. Electrochemical and Solid-State Letters, 2008, 11, K98.	2.2	20
164	Effect of Additives on Shape Evolution during Electrodeposition. Journal of the Electrochemical Society, 2007, 154, D584.	1.3	43
165	Plasma-enhanced chemical vapour deposition growth of Si nanowires with low melting point metal catalysts: an effective alternative to Au-mediated growth. Nanotechnology, 2007, 18, 505307.	1.3	120
166	Plasma assisted growth of nanotubes and nanowires. Surface and Coatings Technology, 2007, 201, 9215-9220.	2.2	26
167	Quantifying Electrochemical Nucleation and Growth of Nanoscale Clusters Using Real-Time Kinetic Data. Nano Letters, 2006, 6, 238-242.	4.5	248
168	Electrochemical Characterization of Adsorption-Desorption of the Cuprous-Suppressor-Chloride Complex during Electrodeposition of Copper. Journal of the Electrochemical Society, 2006, 153, C258.	1.3	56
169	The morphology and nucleation kinetics of copper islands during electrodeposition. Surface Science, 2006, 600, 1817-1826.	0.8	116
170	Underlayer effects on texture evolution in copper films. Thin Solid Films, 2006, 503, 207-211.	0.8	8
171	Nucleation and Growth Study of Nickel Nanoparticles on Silicon ECS Transactions, 2006, 2, 409-416.	0.3	5
172	The chemistry of additives in damascene copper plating. IBM Journal of Research and Development, 2005, 49, 3-18.	3.2	407
173	Electrodeposition of bismuth thin films on n-GaAs (110). Applied Physics Letters, 2005, 86, 121916.	1.5	29
174	Dynamic microscopy of nanoscale cluster growth at the solid–liquid interface. Nature Materials, 2003, 2, 532-536.	13.3	683
175	Liner materials for direct electrodeposition of Cu. Applied Physics Letters, 2003, 83, 2330-2332.	1.5	154
176	Electrodeposition of Bi[sub 1â^'x]Sb[sub x] Thin Films. Journal of the Electrochemical Society, 2003, 150, C131.	1.3	14
177	Electrochemical Deposition of FeCo and FeCoV Alloys. Journal of the Electrochemical Society, 2003, 150, C184.	1.3	30
178	Synthesis and Characterization of Particle-reinforced Ni/Al <sub>2</sub> O <sub>3</sub> Nanocomposites. Journal of Materials Research, 2002, 17, 1412-1418.	1.2	68
179	Kinetics of Particle Codeposition of Nanocomposites. Journal of the Electrochemical Society, 2002, 149, C610.	1.3	73
180	Electrochemical Deposition of Bi on GaAs(100). Journal of the Electrochemical Society, 2001, 148, C733.	1.3	18

#	Article	IF	CITATIONS
181	Magnetotransport properties of bismuth films on p-GaAs. Journal of Applied Physics, 2000, 88, 6529-6535.	1.1	43
182	Particle Codeposition in Nanocomposite Films. Journal of the Electrochemical Society, 2000, 147, 2572.	1.3	110
183	Electrochemical formation of GaAs/Bi Schottky barriers. Applied Physics Letters, 1999, 75, 3135-3137.	1.5	19
184	Electrochemical Deposition of Copper on n‣i/TiN. Journal of the Electrochemical Society, 1999, 146, 1436-1441.	1.3	117
185	Electroreduction of Co2 +  and Ni2 +  at III-V Semiconductors and Properties of the Semiconductor/Metal Interfaces Formed. Journal of the Electrochemical Society, 1999, 146, 1412-1420.	1.3	9
186	The Electrochemical Behavior of pâ€Type (100) GaAs in Copper Sulfate Solution: Influence of Surface Conditions. Journal of the Electrochemical Society, 1998, 145, 3075-3082.	1.3	2
187	An improved procedure for the processing of chronoamperometric data: Application to the electrodeposition of Cu upon (100) n-GaAs. Journal of Electroanalytical Chemistry, 1997, 433, 19-31.	1.9	26
188	Electrochemical reduction vs. vapour deposition for n-GaAs/Cu Schottky-barrier formation: a comparative study. Journal of the Chemical Society, Faraday Transactions, 1996, 92, 4069.	1.7	10
189	Electrochemical behaviour of (1 0 0) GaAs in copper(II)-containing solutions. Electrochimica Acta, 1996, 41, 95-107.	2.6	21